

to be published in:  
"Precision Instrument Design",  
SPIE Proceedings Vol. 1036,  
Santa Clara, CA, November, 1988.

MLM-3564 (op)

## Automated Dimensional Analysis Using a Light-Sectioning Microscope

MLM-3564 (op)

John Loomis, Allan Lightman  
The University of Dayton Research Institute  
Dayton, OH 45469

CONF-8811254--1

RECEIVED

JUL 22 1988

OSTI

and

Allen Poe, Roger Caldwell  
Mound Laboratories<sup>1</sup>  
Miamisburg, OH 45342

### ABSTRACT

A computer vision system has been integrated with a modified light-sectioning microscope for the quality control and inspection of a machined part whose critical dimensions are in the range of 30 to 300  $\mu\text{m}$ . Height measurements were determined by analysis of the projected light-section line. Transverse measurements were made using the microscope in a traditional configuration with illumination from selected elements of an external LED ring array. The light section irradiance was under computer control to accommodate the spatial variations in surface reflectance whose dynamic range exceeded that of the vision system. Part features are located by the vision system. Edges and line centers are then measured to sub-pixel resolution with a gray-level analysis algorithm.

This paper describes the design and operation of this system. Details of the measurement process and analysis algorithms are provided.

### 1. INTRODUCTION

Quality assurance/control inspection of microscopic parts is usually performed by human inspectors using microscopes and micropositionable platforms for manipulating the object. The result is subjective, depending upon the experience, visual acuity, and state of mind of each inspector. Human inspection does offer the advantage of providing a complex evaluation and shape recognition system (human mind) that can control system adjustments during measurement to optimize the inspection conditions. The computer vision system reported here uses the same microscope as the human inspector, but substitutes a video imaging system and computer logic for the inspector's eyes and brain. A computer vision system has the advantage of working to the same criteria for each measurement, without fatigue, thus yielding a narrower statistical distribution for the measured parameters than is routinely achieved by human inspectors. A feedback loop between the video camera and the lighting permits the computer to adjust the lighting level and lighting source to optimize the conditions for each individual parameter measurement. The system is more than 10 times faster than the human inspector and permits 100% on-line inspection. Furthermore, as the data are already in the computer, real-time statistical process control can be implemented in a straightforward fashion. This paper describes the system and illustrates its operation.

### 2. MEASUREMENT PROBLEM

The goal of the program was to develop a computer vision system capable of measuring dimensions of a product consisting of two shaped copper posts (about 500  $\mu\text{m}$  diameter) protruding 125  $\mu\text{m}$  from a plastic mounting stud.

<sup>1</sup>operated by E.G.&G. Mound Applied Technologies for the U.S. Department of Energy under contract no. DE-AC04-88DP4395

MASTER

DISTRIBUTION OF THIS DOCUMENT IS UNLIMITED

Loomis

1

## **DISCLAIMER**

**Portions of this document may be illegible  
in electronic image products. Images are  
produced from the best available original  
document.**

## **DISCLAIMER**

This report was prepared as an account of work sponsored by an agency of the United States Government. Neither the United States Government nor any agency thereof, nor any of their employees, makes any warranty, express or implied, or assumes any legal liability or responsibility for the accuracy, completeness, or usefulness of any information, apparatus, product, or process disclosed, or represents that its use would not infringe privately owned rights. Reference herein to any specific commercial product, process, or service by trade name, trademark, manufacturer, or otherwise does not necessarily constitute or imply its endorsement, recommendation, or favoring by the United States Government or any agency thereof. The views and opinions of authors expressed herein do not necessarily state or reflect those of the United States Government or any agency thereof.

as illustrated in Figure 1. A scanning-electron-microscope picture of the part is shown in Figure 2. The two posts are separated by 500  $\mu\text{m}$  and all dimensions are referenced to a line tangent to the plastic surface and extending through the center of the post. The allowed dimensional tolerances ranged between  $\pm 5$  and  $\pm 10 \mu\text{m}$  depending upon the particular dimension and it was desired to achieve a measurement accuracy and repeatability of one-tenth the tolerance.

### 3. EQUIPMENT

The measurement system is shown in Figure 3. The part is viewed through a commercial light-sectioning microscope. A CCD camera is mounted on the microscope's viewing port. The video image is sent to a computer, where it is captured and analyzed. The part is moved under computer control and the illumination is also under computer control. The following sections describe the components of the measuring system in more detail.

#### 3.1 Light-sectioning Microscope

The light-sectioning microscope provides 100 X or 200 X magnification (preselectable) on direct view, and the lens that relays the image to the camera provides an additional 2 X magnification. The horizontal field of view through the video camera using the 100 X objective is 750  $\mu\text{m}$ .

The light-sectioning system is illustrated in Figure 4 along with an example of the contour that would be imaged for a simple part. A "thin" sheet of light is projected onto the sample at 45° to the vertical and the illuminated sample is viewed at the complementary angle about the vertical. As a result the sample is viewed from a perspective of 45° but the illuminating light sheet is perpendicular to the viewing direction. As a result of the configuration a full horizontal cross-section of the object will be observed in focus, with a bright line superimposed on the image. This line, or light-section, effectively sections the sample and, for an opaque sample, the resulting image is a contour of the sample surface in the plane of illumination. Moving the sample across the measurement plane will result in the presentation of successive sections which can be combined to produce a 3-D profile of the part.

The light sheet which performs the sectioning intersects the object over a distance determined by the size of the object. It is necessary that the light sheet remain in acceptable focus over this range so that the measurements can be made to the required accuracy. Enhanced depth of field is achieved by adjusting the aperture of the optical system forming the light sheet. Unfortunately this also reduces the amount of light in the sheet, which was originally provided by a 6 W tungsten bulb. To achieve adequate illumination for a video camera, the original lighting system was replaced. A fiber-optic bundle was used to bring light from a 150 W quartz halogen bulb to the illumination port. The resulting improvement is due to both the increased power and the higher color temperature of the filament. The fiber bundle also isolates the microscope from the light bulb, thereby eliminating thermal problems due to the increased power.

In the original system the slit imaged to form the light sheet is made on a piece of green glass. This filters the illumination, possibly reducing chromatic aberrations, and illuminates the object in the wavelength region optimized for human observation. Since the CCD camera is more sensitive in the near infrared, the original slit was replaced by a clear slit made by photographic reduction. A series of interchangeable slits were produced so that an optimum slit width could be selected.

#### 3.2 Camera

The camera selected for this application was a CCD array (510 x 492 elements) with enhanced sensitivity over standard CCD arrays (minimum illumination of 0.004 fc at the sensor). It is sufficiently light that the vertical adjustment drive can support it without external aid. Using the 100 X objectives yielded a magnification of 1.5  $\mu\text{m}$  per pixel horizontally and 0.86  $\mu\text{m}$  per pixel vertically.

### 3.3 Variable Lighting

The reflectivity of the metal and plastic surfaces of the part varied greatly, and the resulting light levels extended well beyond the dynamic range capability of the video camera. Furthermore, the received illumination changed dramatically from point to point in regions of the same material. Part of the variation is due to the contour of the object and part is a result of the microscopic machining marks left when the contour is cut. Both can act as facets producing glare when viewed in the direction of reflection. The plastic stud was a dark diffuse reflector much weaker than the bright copper, but it formed the datum position from which all height measurements were referenced. To acquire both the contour and the datum in one pass, a light intensity controller was implemented. One port of an I/O board on the computer was dedicated to interfacing to this controller providing an 8-bit control. The system is shown in Figure 5. The computer determines the phase of the applied voltage at which the lamp is turned off, adjustable to 1 part in 256 (8 bits). The lamp intensity is non-linearly related to the phase of the applied power and this provides enhanced control at the lower intensity levels where it is required.

The edge contouring also complicates the determination of edge locations introducing errors in the cross-field dimensions. A critical dimension in this program was the width of a slot in the copper. Locating the vertical side-walls proved impossible with the light-sectioning illumination. An alternate light source, composed of ultra-bright LEDs (2000 mcd), was arranged in a ring mounted on one of the microscope objectives and pointed at the sample. Symmetrically placed pairs of LEDs could be individually turned on/off under computer control. The lighting was arranged to show the slot in relief and the dimension of the width was obtained in that configuration.

### 3.4 Translation Stage

The samples were mounted in a holder on top of a motorized micropositionable drive. This allowed the sample to be driven through the measurement volume to locate the centers of the posts. To measure the slot width, the part was moved until the edge of the post was in focus and the slot could be viewed directly from the 45° observation direction. The translation stage was controlled from the computer over an RS-232 interface. Positioning accuracy was within 0.1  $\mu$ m.

### 3.5 Computer System

The prototype computer system consisted of a host computer, serial interface, parallel-I/O interface, and a video imaging system with frame-grabber and frame buffer. RS-170 video signals are digitized by the frame-grabber and displayed on an auxiliary monitor. The images are 512 x 480 arrays of 8-bit pixels (256 gray levels).

All software was written in the C language.

## 4. PROCEDURE

The following sections discuss the measurement process, the method used for geometrical calibration, and the algorithm used to find edges in digital images.

### 4.1 Measurement Process

The measurement process is started by an operator who inserts the part in an inspection jig that centers the plastic mounting stud and holds the plastic surface against a fixed reference surface. The mechanical tolerances are such that no adjustments are usually required for focus, alignment, or position. A live video signal is provided so that the operator may verify part placement while the system waits for the operator to enter a part number. This entry

signals the start of the automatic inspection sequence. The system locates the light-section line on the plastic and then measures the two posts. Each post is first positioned so that the light-section line bisects the post. Then the slot depth, width, height, and centering are determined. The results are stored on a data file for use by a statistical process control program.

The digitized image of a post with the light-section line crossing the middle of the post is shown in Figure 6(a). Passing the image through an edge-extraction algorithm produces a geometric rendering of the boundaries of the light section, shown in Figure 6(b). This step represents an abstraction from image representation (pixel values) to a geometric representation (line coordinates). A schematic of the components of the light section is shown in Figure 6(c). The light section is generally focused near the machined base of the post. Using a narrow slit to obtain the desired resolution in the light-section leads to a depth of focus shallow enough that the plastic reference line and the line intersecting the top of the slot are blurred. Even when the light-section is sharply focused on a particular plane, irregular surface structure distorts the line image. Reflections out of the plane of observation (which is perpendicular to the light-section line), such as along the walls of the slot or the sloping base, are greatly attenuated from the specular components, and are generally not visible in the video image.

Generally the diffuse reflectance of the part is low enough that only the light-section is visible in the image. The light level must be adjusted to prevent saturation of the video signal (digitized values less than 255). A small area in the upper-left corner of the screen is examined to determine if the background level is acceptable. Background pixel values of about 50 are typical. Next a long vertical strip at the left side of the screen is examined to find the light-section on the plastic stud. We look for regions exceeding a preset threshold. Failure to find the light-section implies a system problem, such as a burned-out bulb. The software generates an error message and terminates the measurement process. Once the light-section is located, the edge algorithm to be described later is used to find its edges near the left and right sides of the screen, and a reference line is fitted to this data.

The inspection jig is adjusted so that when the part is first viewed, the light-section line falls between the two metal posts. After the plastic reference line has been established, the part is translated in small steps ( $50 \mu\text{m}$ ) until the light-section is observed to intersect the base of the upper post. A rectangular region of the image above the reference line is checked for the presence of the light-section. The algorithm used determines the rectangular extent of the region above threshold. Consider the irregularly shaped light blob shown in Figure 7. The rectangular extent is the smallest rectangle that just surrounds the light blob. It can be found by noting the minimum and maximum coordinates for pixels exceeding the threshold value. The algorithm returns the number of pixels above threshold. This number is zero unless the light-section is present.

After the post has been detected, the left side of the base light-section (see Figure 6c) is tracked as the part is moved in  $10 \mu\text{m}$  steps until the midpoint of the base is located. The rule used is that the left side of the light-section extent line takes on its smallest left-most value at the mid-point of the post. Equivalently, we could, of course, have chosen to check for the largest right-most value. At this point in the measurement process, we have located the post and identified the left side. Failure to find the post means the part is defective. An error message is generated and the measurement is terminated.

The extent algorithm used in finding the post does not locate the edges of the light-section to great precision. However, the algorithm is very fast because arithmetic operations are not required. This is a distinct advantage since a sequence of images are acquired as the position of the part is varied. Great precision is not needed at this stage of the measurement.

Once the part is moved, the plastic datum line may shift in the video image, so the reference line must be established again. A least-squared-deviation linear fit is taken through the edge coordinates. Although the width of the light-section may be broadened by defocusing, the center should be located in the same place. Furthermore, since both sides of the light-section are broadened the same way, the center location does not depend on the threshold level used to determine the edges.

As described earlier, if the light level was set at the appropriate value for the metal, the level would be too low for the plastic. This led to the incorporation of the light-level control circuit. At first it seemed desirable to control the light-level dynamically by monitoring the average reflectance as a function of light-level. However, we

discovered that there is a time constant of about 0.1 sec in the response of the light to changes in the control level. Therefore, it was decided to use fixed control levels for metal and plastic materials, determined experimentally, rather than to use a time-consuming search algorithm.

After measuring the plastic datum line, we measure the location of the bottom of the slot. This is determined by the centroid of the light-section spot and marked by a small cross-hair on the screen, as shown in Figure 8. The edges of the spot are outlined in color on the displayed image. The edge finding algorithm, to be described later, allows the centroid to be found within a fraction of a pixel. The distance of the centroid above the reference line is the slot height.

The slot top is measured by fitting a straight line through the left and right parts of the top light-section, as defined in Figure 6(c). The vertical distance of the slot-bottom centroid to this line is the slot depth.

The centering of the slot is determined by comparing the slot centroid to the center of the post, halfway between the left and right extents of the line through the base of the post.

The measurements so far used vertical distances between segments of the light-section. Determining slot width requires a horizontal distance measurement. In this mode, the microscope is used as a traditional machinist's distance-measuring microscope. Furthermore, since the top of the slot is somewhat contoured, it does not provide a distinct edge on which to base a measurement. However, if the post is translated so that the ends of the slot are in focus, there are reasonably high-contrast edges to use for a width measurement, provided that the edges are properly illuminated. Examples of these edges are shown in Figure 9. Auxiliary lighting, consisting of super-bright LEDs, was added to enhance the edge contrast.

In translating to the proper position for a width measurement, we found that we could track the light-section at the top of the slot until it just disappeared. The edge of slot ends would then be in focus a fixed distance below the top of the slot. Typically, the outside of the slot is near background illumination level while the inside of the slot is brightly illuminated. The first vertical edges encountered approaching the slot from the left and then from the right are used as the boundaries of the slot. The horizontal distance between these edges is the slot width.

Measurement of slot width completes the measurement process for one post. An identical process is used for the second post to complete the entire measurement of one part.

#### 4.2 Geometric Calibration of Camera Field of View

The magnification of the digitized video image was determined by viewing a microscope stage calibration scale, marked at intervals of  $50 \mu\text{m}$ . The edge and center locations of a cross-section of the scale were obtained. Measurements were made with the scale oriented horizontally. Because of the geometry of the light-sectioning microscope, the vertical depth of focus limits view to a horizontal strip across the calibration scale.

The camera field of view is digitized into a  $512 \times 512$  pixel array in the frame buffer, but the magnification is different for horizontal and vertical directions. Separate calibrations are made for the horizontal and vertical array directions by rotating the camera  $90^\circ$  between calibrations. A least-squares-deviation line is fitted to the pixel edge coordinates versus the scale reading. The slope of this line is the geometric calibration factor. The results were a scale of  $1.50 \mu\text{m}$  per pixel for the horizontal image direction and  $1.21 \mu\text{m}$  per pixel for the vertical image direction.

A fixed factor of 0.707 must be applied to the vertical scale to account for the  $45^\circ$  oblique viewing direction. The final sensitivity for height measurements is  $0.855 \mu\text{m}$  per pixel.

### 4.3 Edge-finding Algorithm

An ideal edge is the locus of points marking an abrupt change in luminance, color, or texture. Figure 10 shows the video image of a luminance edge. Individual pixels are shown as small squares of constant luminance. Edges may be defined numerically by their location, magnitude, and orientation. In Figure 10, the endpoints A and B are ordered such that the higher luminance is to the right of the edge.

We have adopted the concept of an edgel as the smallest component of an edge. We define an edgel as a directed line segment lying within a pixel and formed by the intersection of the edge center line with the pixel, as shown in Figure 11. The direction is chosen such that the region of higher luminance is to the right. An edgel, therefore, can be identified by its intersections with the pixel boundaries. These end-points define both the location and orientation of the edgel.

Edges are modeled by fitting a plane to the neighborhood of each pixel. The equation of the plane is

$$z = c_x x + c_y y + c_z$$

where  $z$  is the pixel luminance.

Our choice of neighborhood is based on a mask two pixels square and centered over the pixel under investigation, as shown in Figure 12. Each pixel covered by the mask is weighted in proportion to the area covered. The resulting  $3 \times 3$  array of weights is used in constructing the least-squares fit to the plane.

The equation of the plane can now be expressed as

$$2s_x x + 2s_y y + s_z = 16z.$$

Each coefficient in this equation is an integer equal to the convolution of a  $3 \times 3$  array centered on the pixel under investigation. These convolution arrays are shown in Figure 14. By design, the arrays for the coefficients  $s_x$  and  $s_y$  correspond to the Sobel edge operators.

The locus of points on the plane for which the luminance equals the threshold luminance is the threshold line. If the threshold is  $z_t$ , the threshold line is given by

$$s_x x + s_y y = d/2$$

where  $d = 16z_t - s_z$ . If the threshold line crosses the central pixel, its intersections with the pixel boundaries define an edgel. The line through the center pixel in figure 12 is the edgel for that pixel. The problem of finding the intersection points is identical to that in computer graphics of clipping a line at a rectangular window. There are at most two intersections of the threshold line with the pixel. These intersections are the endpoints of the edgel.

The sub-pixel line shown in Figure 13 is the result of drawing the edgel line within each enlarged pixel square. Each edgel is determined independently, but each blends smoothly into the next to form a continuous line. For this example, the scale is too small to reveal the discontinuities between the edgels.

## 5. RESULTS

A comparison between human and machine inspection was performed for the same part. Manual measurements were made using the reticle and micrometer head on the light-sectioning microscope. The dial resolution was  $1 \mu\text{m}$ . The vision system then measured the same part. Agreement within about  $1 \mu\text{m}$  was obtained for slot depth and height and about  $2 \mu\text{m}$  for slot width. The slot width measurement is the most difficult because of differences of operator opinion on exactly where the edges are located.

Multiple runs on the same part with the vision system resulted in a reproducibility of about  $0.2 \mu\text{m}$  in slot depth and height and about  $1 \mu\text{m}$  in slot width.

Total measurement times of 45-60 seconds per part were achieved with the prototype vision system. This included measurement of all dimensional features on both posts. Typical manual inspection required 3-5 minutes per part, but involved quantitative measurements only for some dimensional features and only on one post.

Loomis

## 6. CONCLUSIONS

A computer vision system for inspection and dimensional analysis of microscopic parts has been described. The system achieved its goals of performing measurements faster than human inspectors did and with greater consistency. The system was designed to allow multiple lighting options, selected by the computer according to the particular parameter being acquired. The software design was specialized for the part being measured. This enhances the system performance at the cost of focusing the operation on a limited class of objects. We believe that this customization will probably be necessary for most computer vision systems to achieve a robust measurement system. The computer data interpretation permits measurement enhancements through data interpolation and the algorithms used in this system show promise for application to the general class of vision problems where locating edges is required.

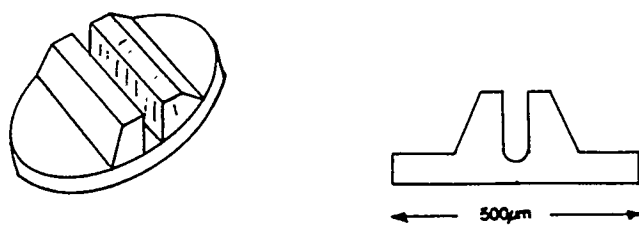


Figure 1: Shape of machined slot inspected by vision system.

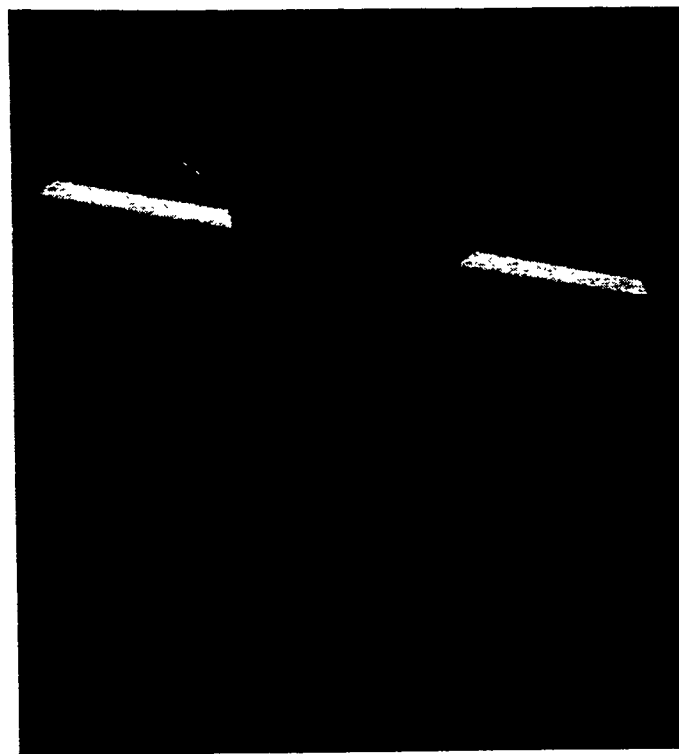


Figure 2: Scanning-Electron-Microscope image of machined metal posts embedded in plastic.

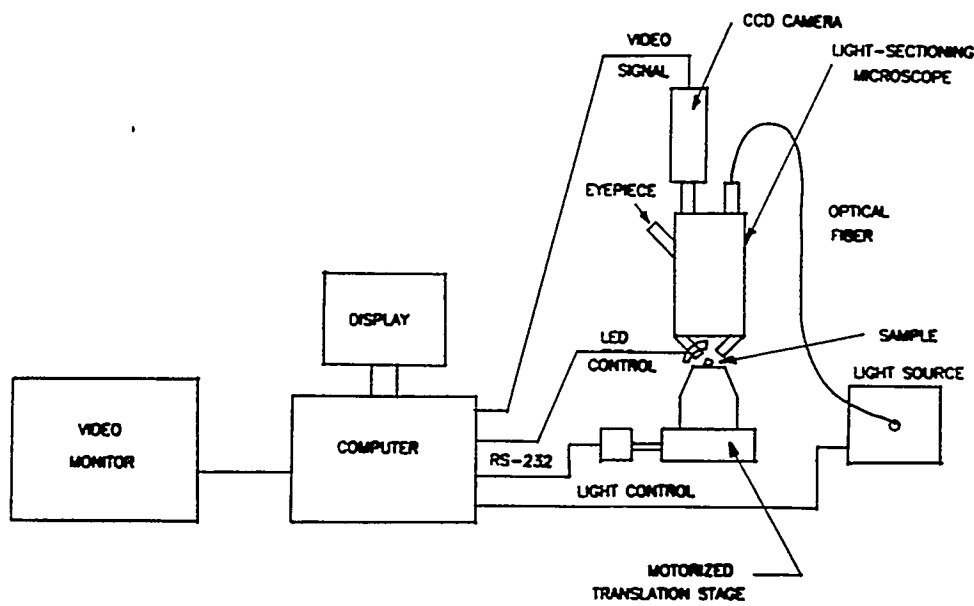


Figure 3: Diagram of measurement system.

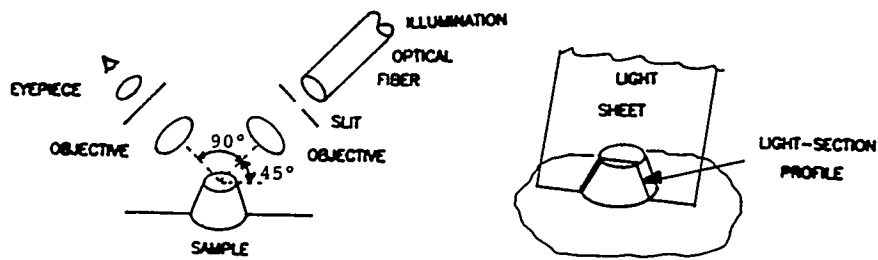


Figure 4: Light-sectioning microscope operation.

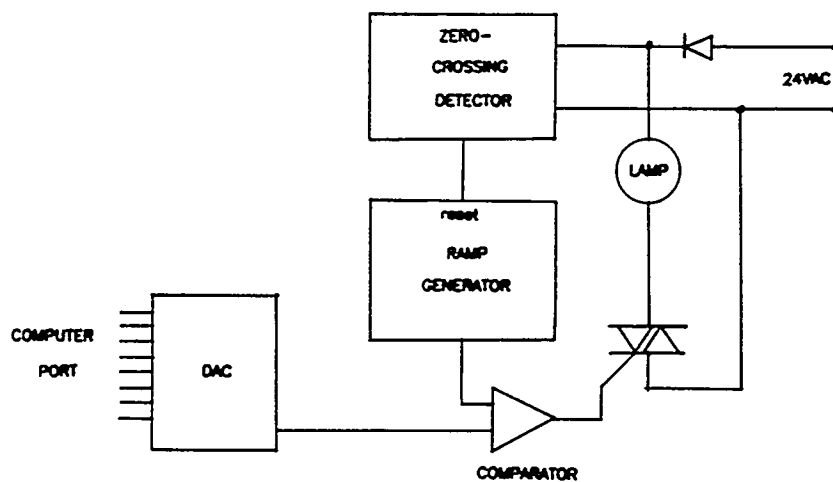


Figure 5: Power controller for fiber-optic light source.

Lionni

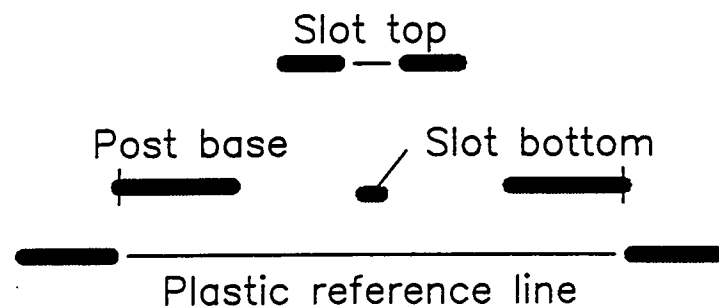
9



(a) original image of light section



(b) geometric edges of light section



(c) schematic diagram of light section

Figure 6: Intersection of light-section line with a typical part.

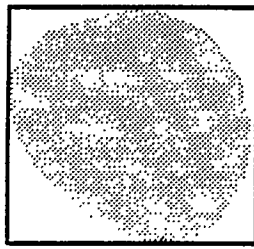


Figure 7: Rectangular extent of irregular spot.

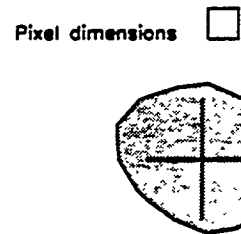


Figure 8: Centroid of light-section at bottom of slot.

Leomis

15

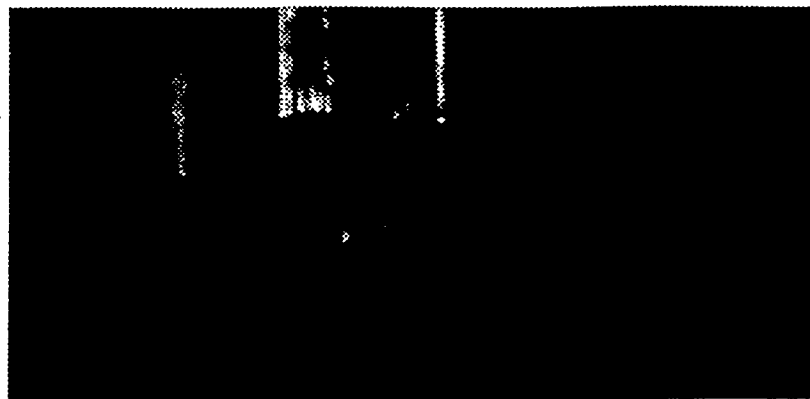


Figure 9: Example of image of slot end.

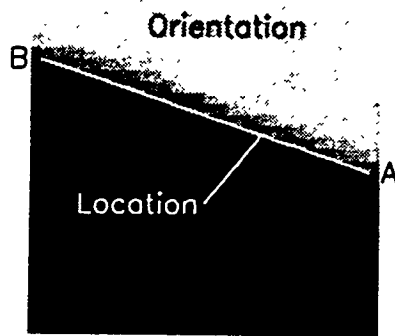


Figure 10: Magnified image of digitized edge.

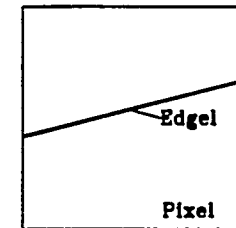


Figure 11: Definition of an edgel.

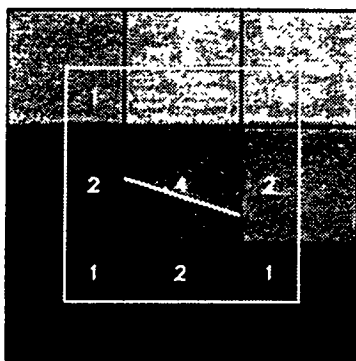


Figure 12: Pixel weight array.

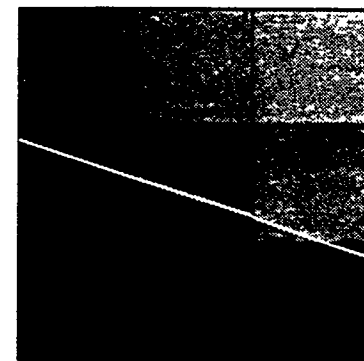


Figure 13: Sequence of edgels.

-1	0	1
-2	0	2
-1	0	1

1	2	1
0	0	0
-1	-2	-1

1	2	1
2	4	2
1	2	1

Figure 14: Convolution masks used in fitting a plane to the neighborhood of a pixel.